TIMOTHY D. STARK, Ph.D., P.E., BC.GE

Stark Consultants, Inc., 401 W. Indiana Ave., Urbana, Illinois, 61801; tstark32@gmail.com; (217) 840 - 8263

To: Mr. Ethan Eberly
Ms. Jessica Russell
Weston Solutions, Inc. (WESTON)
1400 Weston Way
West Chester, PA 19380

From: Timothy Stark, Ph.D., P.E., BC.GE, Dist.M.ASCE

Date: July 2, 2024

RE: Review Comments on May 7, 2024 GLA Report on West and North Slope Stability Analysis Update for Chiquita Canyon Landfill

---

Pursuant to your request, I have reviewed the report titled: "West and North Slope Stability Analysis Update" prepared by Geo-Logic Associates (GLA) and dated May 2024. This memo presents my comments on the GLA analyses as part of my contract requirements with WESTON. The main objective of this review is to develop viable slope stability analyses to assess the current and future stability of the landfill slopes along the west and north sides of Chiquita Canyon Landfill (CCL) located at 29201 Henry Mayo Drive in Castaic, California.

The subject GLA report was prepared to respond to the March 22, 2024 letter to CCL from the Los Angeles County Department of Public Health in its role as the Local Enforcement Agency (LEA). The LEA letter appended a March 12, 2024 letter from Todd Thalhamer of CalRecycle that included a series of comments and requirements based on his review of the information in the February 2024 Stability Analysis Report (GLA, 2024) that was prepared to address the stability analysis requirements in LEA/CalRecycle November 2023 letters to CCL.

Landfill Location and Description:

Figure 1 presents an aerial view of the CCL and the area of the west and north slopes, which are the subject of the GLA May 7, 2024 report (see dashed red box). CCL is a Class III non-hazardous municipal solid waste (MSW) landfill. The 639-acre landfill site began accepting waste in 1972. The landfill can receive up to 12,000 tons of MSW per day. The average daily tonnage in 2021 was reported to be 6,412 tons. The CCL only accepts non-hazardous solid waste for disposal, including municipal solid waste, green waste for composting or recycling, construction and demolition debris, and e-waste for recycling.

The landfill site is a former limestone quarry, which began in 1939 and ended in 1988. The quarrying resulted in two quarry pits, the North Quarry Pit and the South Quarry Pit, which were excavated to maximum depth of 240 feet below ground surface (bgs). The north and south quarry portions cover an area of approximately 52 acres. Landfilling began in the North Quarry Pit in

1974 and continued in this area until 1985. In 1985, the landfill underwent expansion to the southwest into the area known as the South Quarry Pit.



Figure 1. Google Earth aerial photo on February 14, 2024 of landfill showing site visit area (see dashed red rectangle), western slope toe covered with black tarp, and white geomembrane covering a portion of the northwest slope.

The total waste thickness is approximately 320 feet which means about 80 ft is above ground surface and about 240 feet is below ground surface. The landfill accepted approximately 17,000,000 in-place cubic yards of waste, including commercial, and municipal solid wastes. The permitted landfill disposal footprint totals 257 acres and is comprised of three separate areas designated as "Primary" Canyon, "Canyon B", and the Main Canyon (including Canyons A, C, D and subsequent fill modules). Currently, 231 acres of the footprint have been used for disposal. All areas except the Primary Canyon have geosynthetic bottom liner systems and leachate

collection and removal systems. Leachate is collected and trucked off site but condensate from the gas extraction wells is injected into the flare.

Review Comments on May 7, 2024 GLA Stability Report:

This section provides my review comments on the GLA report titled: "West and North Slope Stability Analysis Update" and dated May 2024. Each subsection presents my comments on the corresponding section of the subject GLA Report.

3.1 Surface Conditions

As stated in my CCL site visit report dated July 2, 2024, I observed tension cracks along the western slope. For example, I observed a gas extraction well being pulled downslope from the upslope interim cover soil leaving a tension crack just above the gas well. This and other observations indicate the western slope was undergoing slope movement on May 23, 2024.

This is in agreement with GLA's statements in Section 3.1 that their slope profiles continue to show evidence of lateral displacement between about the first and second benches on the western slope. The displaced material did not extend a significant distance beyond their cross-section WS-A to the north and WS-C to the south. GLA concludes the slope movement is due to excavation of the toe of the slope but I think elevated gas and liquid pressures from the Subsurface Elevated Temperature (SET) Event are contributing to the slope movement and the fluid or "oozing" nature of the waste along the western slope toe.

As a result, I disagree with GLA's statement that there is "no evidence of the surface features that would be expected if the slope had been affected by a slide". Even with the black scrim in-place along the toe of the western slope there is evidence of slope movement above the excavated toe area as described in my July 2, 2024 site visit report.

3.2.1 Cross-Sections

This section provides my review comments on cross-section WS-A, WS-B, WS-C, WS-D, and WS-E used in the slope stability analyses conducted by GLA and discussed in their May 2024 report titled: "West and North Slope Stability Analysis Update".

A total of eight cross sections were created and analyzed by GLA but sections WS-A, WS-B, WS-C, WS-D, and WS-E through the western slope are the most relevant given the current position of the Subsurface Elevated Temperature (SET) Event as of my site visit on May 23, 2024. **Figure 2** shows the location of the eight cross sections created by GLA for their slope stability analyses. It is anticipated that cross-section WS-E, also through the west slope, will be important in the near future due to the southward migration of the SET Event.

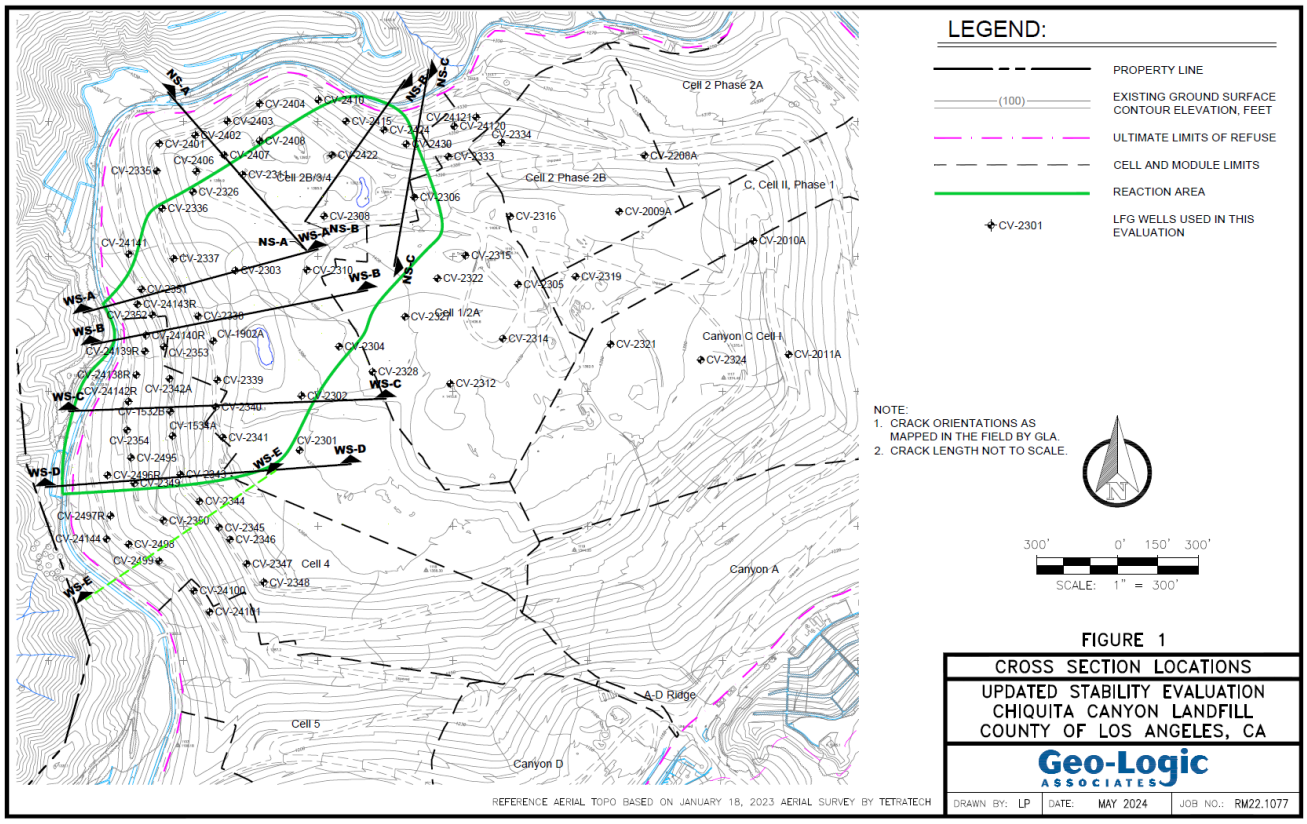


Figure 2. CCL Plan View and Cross-Section Locations in Figure 1 from GLA Report dated May 2024.

My review comments on these five west slope cross-sections are listed below:

1. Figure 2 of the May 2024 GLA Report shows cross-sections WS-A, WS-B, and WS-C. All of these cross-sections show the "well degraded MSW" decreasing in thickness between the available borings as shown in **Figure 3** below. The thickness of the "well degraded MSW" could be as deep as shown near the borings or even deeper, which may impact the location and shape of the critical failure surface. This is important because the factor of safety (FoS) varies with each failure surface analyzed. In addition, GLA admits the "base of degraded MSW" is not known and is approximated so a conservative thickness should be evaluated in their analyses. This would account for the uncertainty in the value of FoS due to the thickness of degraded or charred waste.

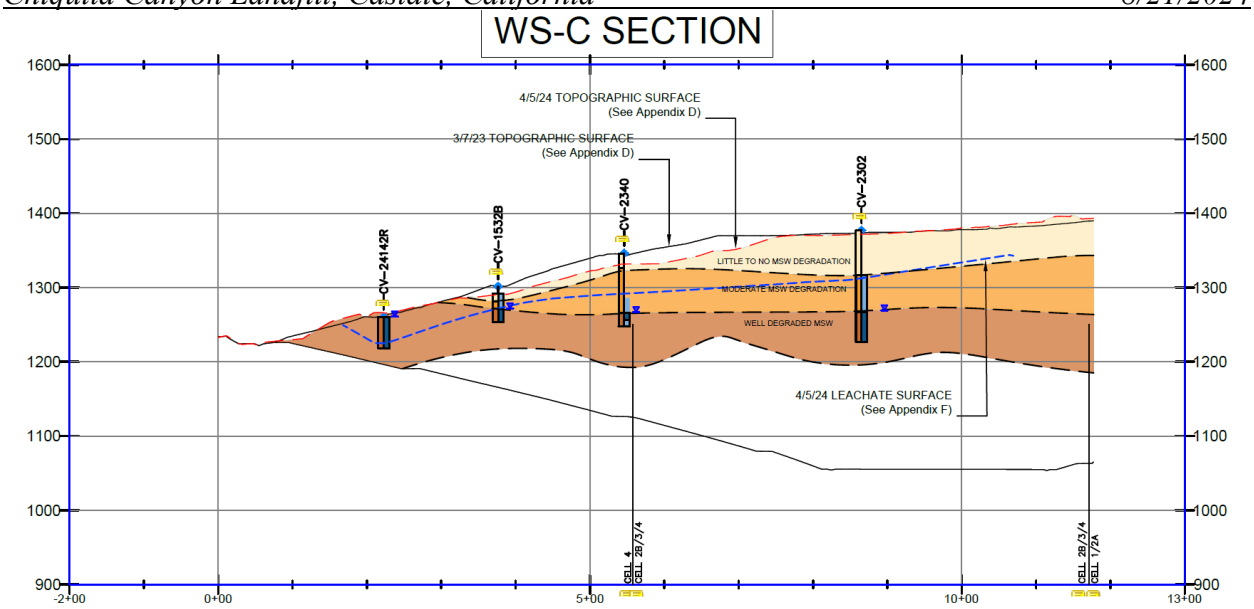


Figure 3. Cross-Section WS-C in Figure 2 from GLA Report dated May 2024.

3.2.2 Methods

This section provides my review comments on GLA's slope stability method and results. In particular, GLA states that both Morgenstern and Price (1965) and Spencer (1967) slope stability methods "gave essentially the same answer", but the Morgenstern and Price (1965) was used to calculate the reported values of FoS. Spencer's (1967) method is a simplification of the Morgenstern and Price (1965) method and usually yields the same answer if the user selects Spencer's (1967) Method or the "constant" interslice force function for the Morgenstern and Price (1965) method. It is recommended that all of the interslice force functions, e.g., trapezoid, half-sine, and clipped sine, be used for the critical failure surface and report the lowest FoS for future GLA analyses. This accounts for the uncertainty in the calculated value of FoS, which is different than the uncertainty in the input parameters discussed below.

3.2.3.2 Liner Materials

The bottom and side slope liner systems in Cell 1/2A and Modules 2B/3/4 P2, 2B/3, and 4 are shown in **Table 1** and generally consist of a single composite geosynthetic liner system comprised of a 60 mil thick HDPE geomembrane underlain by a geosynthetic clay liner (GCL).

TABLE 1. SUMMARY OF BOTTOM LINER SYSTEMS INVOLVED IN SET EVENT AT THE CCL

Bottom Liner System	Side Slope Liner System
Cell 1/2A	
Soil Operations Layer	Soil Operations Layer
Granular Leachate Collection System	Nonwoven Geotextile in Upper 1/3 of Slope
Double-Sided Textured 60 mil thick HDPE Geomembrane	Single-Sided Textured-Down 60 mil thick HDPE Geomembrane
Geosynthetic Clay Liner (GCL)	GCL
Smooth Wheel Compacted Subgrade	Smooth Wheel Compacted Subgrade
Modules 2B/3/4 P2, 2B/3, and 4	
Soil Operations Layer	Soil Operations Layer
Geosynthetic Drainage Composite	Geosynthetic Drainage Composite
Double-Sided Textured 60 mil thick HDPE Geomembrane	Double-Sided Textured 60 mil thick HDPE Geomembrane
Geosynthetic Clay Liner (GCL)	
Smooth Wheel Compacted Subgrade	Smooth Wheel Compacted Subgrade

GLA states that it used large displacement (LD) interface strengths instead of residual interface strengths as recommended by Stark and Poeppel (1994). GLA used LD strengths probably because they conducted interface direct shear tests, which do not impart enough displacement to reach the residual condition. However, GLA can extrapolate their direct shear test results using the procedure outlined by Lin et al. (2024). This is recommended because the western slope cannot limit the amount of shear displacement that it undergoes to reflect the one to three inches of shear displacement that a direct shear device can impose.

Use of the residual interface strength is recommended because the field critical failure surface could involve a portion of the bottom liner system. In addition, the following analyses in Appendix G of the GLA May 2024 report show the predicted critical failure surface does involve a portion of the bottom liner system:

1. NS-A (R1A).slmd
2. NS-B (R1A).slmd
3. NS-C (R1A).slmd
4. WS-B (R1A).slmd
5. WS-C (R1A).slmd (see **Figure 3**)
6. WS-D (R1A).slmd
7. WS-E (R1A).slmd

For example, **Figure 4** presents the slope stability analysis for Slope Stability Analyses for Cross-Section NS-C using degraded MSW strength parameters that is presented in Appendix G of the GLA Report dated May 2024. **Figure 4** shows the critical failure surface, see red line, that yields the lowest static FoS of 2.1. More importantly, **Figure 4** shows the critical failure surface passes from the landfill surface, through the waste and then reaches the bottom liner system. The critical surface follows the bottom liner system to the toe of the slope where the surface ends. If the residual interface strength is applied to the bottom liner system, a lower FoS will be obtained than reported in Table 2 of the May 2024 GLA Report because the residual interface strength is lower than the LD interface strength.

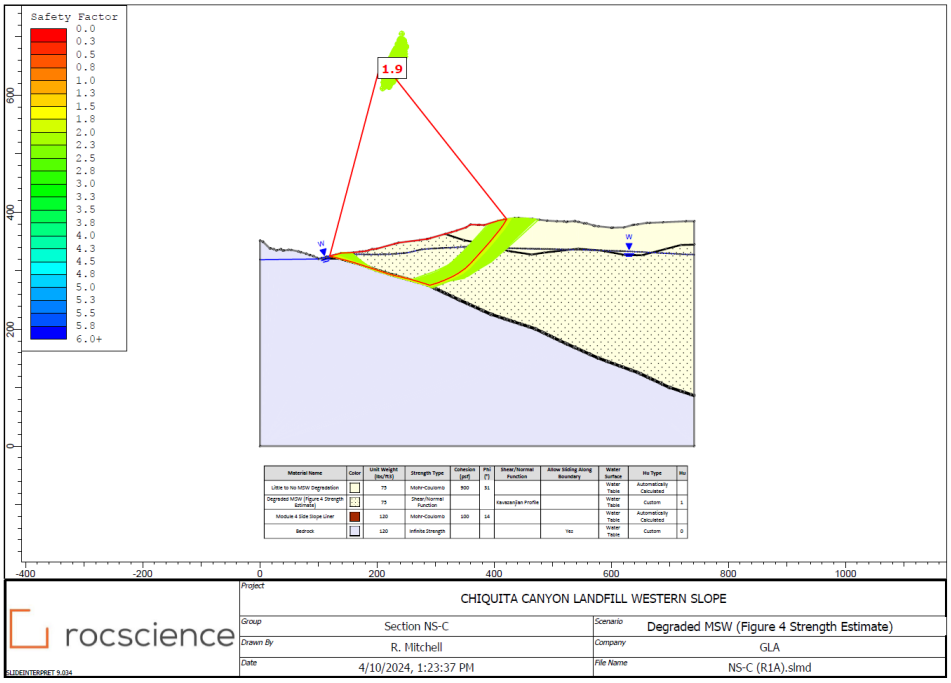


Figure 4. Slope Stability Analyses for Cross-Section NS-C and Degraded MSW Strength Parameters Presented in Appendix G of the GLA Report dated May 2024.

3.2.3.3 Waste Materials

This section provides my review comments on waste shear strength parameters used by GLA in their slope stability analyses presented in their May 2024 report titled: "West and North Slope Stability Analysis Update". My review comments on the selected waste shear strength parameters are listed below:

1. GLA uses shear strength parameters for unaffected (or non-degraded) MSW suggested Kavazanjian et al. (2013). Of course, MSW varies considerably so a range of waste strength parameters should be used and the parameters that yield the lowest FoS should be utilized. Table 1 of the GLA Report summarizes some of the recommended shear strength parameters for unaffected (or non-degraded) MSW but most of the parameters are based on laboratory testing and unfailed landfill slopes so the FoS, and thus the waste parameters, are not known.

   For some reason, GLA omits the waste shear strength parameters based on failed landfill slopes provided by Huvaj and Stark (2008) and Stark et al. (2009), which are probably more representative laboratory tests. The stress-dependent MSW strength parameters recommended by Stark et al. (2009) are:

$0 \leq$ Normal stress $\leq$ 4,200 psf	c' = 125 psf and $\phi' = 35^0$
Normal stress $\geq$ 4,200 psf	c' = 625 psf and $\phi' = 30^0$

   GLA should use available MSW shear strength parameters and determine which set of parameters yield the lowest FoS. This would account for the uncertainty in the value of FoS due to the waste shear strength parameters.

2. GLA mentions the inverse analysis of the Payatas Landfill by Merry et al. (2005) but fails to consider a subsequent inverse analysis by Jafari et al. (2013) that accounts for the gas and liquid pressures present at the time of failure. In particular, rainfall from two recent typhoons and landfill gas from biodegradation caused increased pore pressures within the Payatas Landfill that resulted in a decrease in effective stress and stability. The landfill gas pressure was modeled using an equivalent fluid unit weight that reflects the leachate and gas pressure. The value of equivalent fluid unit weight estimated from inverse stability analyses is about 11.7 kN/m3 for the Payatas Landfill. Jafari et al. (2013) also discuss the uncertainty in the mobilized waste shear strength parameters due to uncertainties in the leachate level, elevated gas pressure, and degraded state of the waste. The degraded waste exhibited a unit weight close to soil, e.g., 100 to 105 pcf, which can impact the calculated FoS. This is important for the CCL because the elevated gas and

liquid pressures are being induced by a SET Event not just pressures from normal waste biodegradation.

3. Determination of the shear strength parameters for affected (or charred) MSW is even more difficult than for unaffected MSW because the level of degradation various depending on the stage of the SET Event impacting the waste. Jafari et al. (2017) describe the progression of the main indicators of elevated temperatures and arranges them in a chronological sequence, as follows: (1) severe increase in odors and emissions; (2) changes in landfill gas composition and waste appearance, e.g., black and/or charred waste; (3) elevated waste and gas temperatures; (4) elevated gas and leachate pressures; (5) increased leachate volume and migration; (6) slope movement; and (7) rapid and unusual settlement of the waste/landfill. The shear strength of the impacted MSW will vary depending on which of the seven stages of the SET Event is being analyzed.

   GLA concludes "degraded" MSW can be represented by effective stress cohesion, c', of 418 psf and friction angle, ϕ', of 28 to 42^0 based on the inverse analysis of the Payatas Landfill slope failure by Merry et al. (2005). The inverse analysis of the slope failure by Jafari et al. (2013) yielded the following strength parameters: c' = 430 psf and $\phi' = 24.7^0$. Given the deep critical failure surfaces shown in Appendix G of the subject GLA report, it is recommended the Jafari et al. (2013) degraded waste parameters also be used for the two layers of degraded waste underlying the unaffected MSW in GLA's cross-sections, see **Figure 3** above. The deep failure surfaces are a concern because of the lower friction angle and the values of c' being similar.

   Unfortunately, use of the Jafari et al. (2013) strength parameters do not account for the uncertainty in the calculated value of FoS due to the uncertainty in the strength parameters for the charred MSW because the Payatas Landfill was not experiencing a SET Event as the CCL is experiencing. The Payatas Landfill was experiencing normal biodegradation and not smoldering.

4. As stated in my CCL site visit report dated July 2, 2024, I observed black and/or charred waste being excavated by drill rigs installing three new gas extraction wells. Jafari et al. (2017) conclude black and/or charred waste is one of the indicators of subsurface smoldering. In addition, photographs in Appendix C of the May 2024 GLA Report show black and/or charred waste being excavated by drill rigs installing other gas extraction wells. The following gas well borings encountered black and/or charred waste based on photographs in Appendix C: CV-2497, CV-24140 (thermometer in one of the photographs shows a waste temperature of over 190^0F), CV-2496, CV-24143, CV-24144, TP-3, and TP-6 below 100 ft.

5. GLA indicates the completely combusted MSW strength parameters presented by Stark et al. (2010) are too low and should not be used. I agree because these are meant to

be the lowest bound and correspond to completely combusted waste versus waste that is experiencing subsurface smoldering, which usually does not yield complete combustion.

3.3 Leachate and Pore-Water Pressures

This section provides my review comments on the leachate/liquid pressures used in the slope stability analyses conducted by GLA and discussed in their May 2024 report titled: "West and North Slope Stability Analysis Update". GLA assumes the leachate surface acts as a phreatic surface so the waste below this surface is assumed to be saturated. This is probably likely given the: (1) elevated liquid pressures, i.e., geysers, (2) condition of the excavated waste during drilling gas wells, and (3) amount of leachate being handled. However, this assumption results in only hydrostatic liquid pressures being applied in the slope stability analyses and does not account for elevated liquid pressures, i.e., pressure heads.

A manifestation of elevated liquid pressure is the occurrence of leachate geysers during drilling operations (see **Figure 5**). Based on field reports, geysers of 15 to 20 ft have been observed at CCL. Therefore, GLA should include a pressure head of 15 to 20 ft in their slope stability analyses where the leachate geysers have been observed. Of course, the location of the geysers will change as the SET Event moves through the landfill. It is typical to see geysers shoot 10 to 30 ft above the interim soil cover during a SET Event (Martin et al., 2013).

The Payatas Landfill case history analyzed by Jafari et al. (2013) demonstrates that leachate rise can contribute more to a landfill slope failure than the selected MSW shear strength properties. Therefore, characterizing and monitoring the liquid pressures in a landfill experiencing a SET Event is necessary to ensure stability. As a result, CCL should consider installing some Geokon high temperature piezometers that have a working range up to 480^0F. This would provide a direct estimate of the elevated liquid pressures instead of estimating them from the downhole temperature measurements and the ideal gas law (discussed next). The increase in temperature causes the increase in liquid and gas pressures, which can cause slope instability. Therefore, it is important to monitor temperatures first to figure where the elevated gas and liquid pressures are being generated. The elevated liquid pressures can be estimated using the ideal gas law but it would be beneficial to actually measure the pressures to reduce some of the uncertainty in the slope stability analyses.

The ideal gas law is PV = nRT, where P is pressure, V is volume, n is the number of molds in the gas, R is the gas constant, and T is temperature. The ideal gas law shows that increases in temperature are directly related to increases in pressure for a given volume of material, e.g., MSW. This increase in pressure reduces the shear strength of the waste by decreasing the effective stress (σ') in the waste, which is the total or overburden stress (σ') minus the gas and liquid pressure (σ') or $\sigma' = \sigma - u$. This explains the importance of measuring the elevated liquid

pressures to confirm the conversion of temperature increases to liquid pressure using the ideal gas law.



Figure 5. Photograph of leachate geyser and personnel in protective clothing (photo from USEPA at https://www.epa.gov/ca/chiquita-canyon-landfill#photos).

3.4 Slope Stability Analysis Results

This section provides my review comments on slope stability analyses conducted by GLA and discussed in their May 2024 report titled: "West and North Slope Stability Analysis Update". I focused my review on cross-section WS-A, WS-B, WS-C, WS-D, and WS-E, which correspond to the western slope.

The results of the slope stability analyses conducted by GLA are presented in their Table 2 and included herein also as **Table 2**. The static values of FoS for cross-sections WS-A, WS-B, WS-C, WS-D, and WS-E, are 1.4, 1.5, 1.3, 1.7, and 1.8, respectively. Using the slope stability input files provided by Richard A. Mitchell of GLA, I was able to reproduce the values of static FoS and critical failure surface for cross-section WS-A, WS-B, WS-C, and WS-D as reported by GLA and presented in **Table 2**. The resulting critical failure surfaces are shown in **Figure 6**. As a result, I was able to use these GLA input files to investigate the impact of elevated liquid pressure on the static FoS below.

Using the slope stability input files provided by Richard A. Mitchell of GLA, a pressure head of 15 ft was applied to the cross-sections WS-A, WS-B, WS-C, and WS-D. The pressure head was applied in each input file the hydrostatic water level was changed to a piezometric line and then the piezometric line was raised by 15 feet. The resulting values of static FoS are shown in **Table**

3. Using an observed geyser height of 15 ft, the static FoS decreased by unity (failure) for cross-sections WS-A and WS-B. This means if the SET Event induces a geyser of 15 ft in a boring near cross-sections WS-A and WS-B, slope instability could occur.

TABLE 2. SUMMARY OF UPDATED SLOPE STABILITY ANALYSES PRESENTED IN GLA'S MAY 2024 REPORT.

Table 2
SUMMARY OF UPDATED STABILITY ANALYSIS RESULTS
Chiquita Canyon Landfill
West and North Slope Evaluation

CROSS SECTION	LEA/CALRECYCLE-SPECIFIED DEGRADED MSW STRENGTH PROFILE		FIGURE 4 DEGRADED MSW STRENGTH PROFILE		SEISMIC DISPLACEMENT (Figure 4 Degraded MSW Strength Profile)					
	Static Safety Factor	Pseudostatic Safety Factor (@ 0.15g)	Static Safety Factor	Pseudostatic Safety Factor (@ 0.15g)	Yield Acceleration (g)	Earthquake	Magnitude	Spectral Acceleration @ $1.5T_s$ (g)	Estimated Displacment (cm)	Estimated Displacement (in)
NS-A	1.0 to 1.5	<1	3.5	2.2	NC	NC	NC	NC	NC	NC
NS-B	1.1	<1	2.6	1.2	0.21	MCE	6.8	1.0	16.6	7
NS-C	1.4 to 1.5	<1	1.9	1.0	0.15	MCE	6.8	0.9	25.5	10
WS-A	<1	NA	1.4	<1	0.10	MCE	6.8	0.5	21.5	8
WS-B	<1	NA	1.5	<1	0.09	MCE	6.8	0.5	25.2	10
WS-C	<1	NA	1.3	<1	0.14	MCE	6.8	1.2	41.2	16
WS-D	1.0 to 1.1	<1	1.7	<1	0.13	MCE	6.8	0.1	<1	<1
WS-E	1.1	<1	1.8	1.0	0.15	MCE	6.8	0.1	<1	<1

NOTES:
1. See Figure 1 for cross section locations.
2. Appendix G for analysis output.
3. All analyses assume a single (non-layered) degraded waste profile that is laterally continous across the section and vertically continuous to the base of the landfill.
4. Seismic displacement based on Bray and Travasarou (2007) with the modifications of Bray and Macedo (2021).
5. Shear wave velocity from Kavazanjian et al. (1996).
6. Spectral acceleration from MCE seismic hazard evaluation (see Appendix G for Spectral Acceleration Plot).
7. NC - Not Calculated (Pseudostatic Saftey Factor is >1.5).
8. NA - Not Applicable (Static Safety Factor is <1).

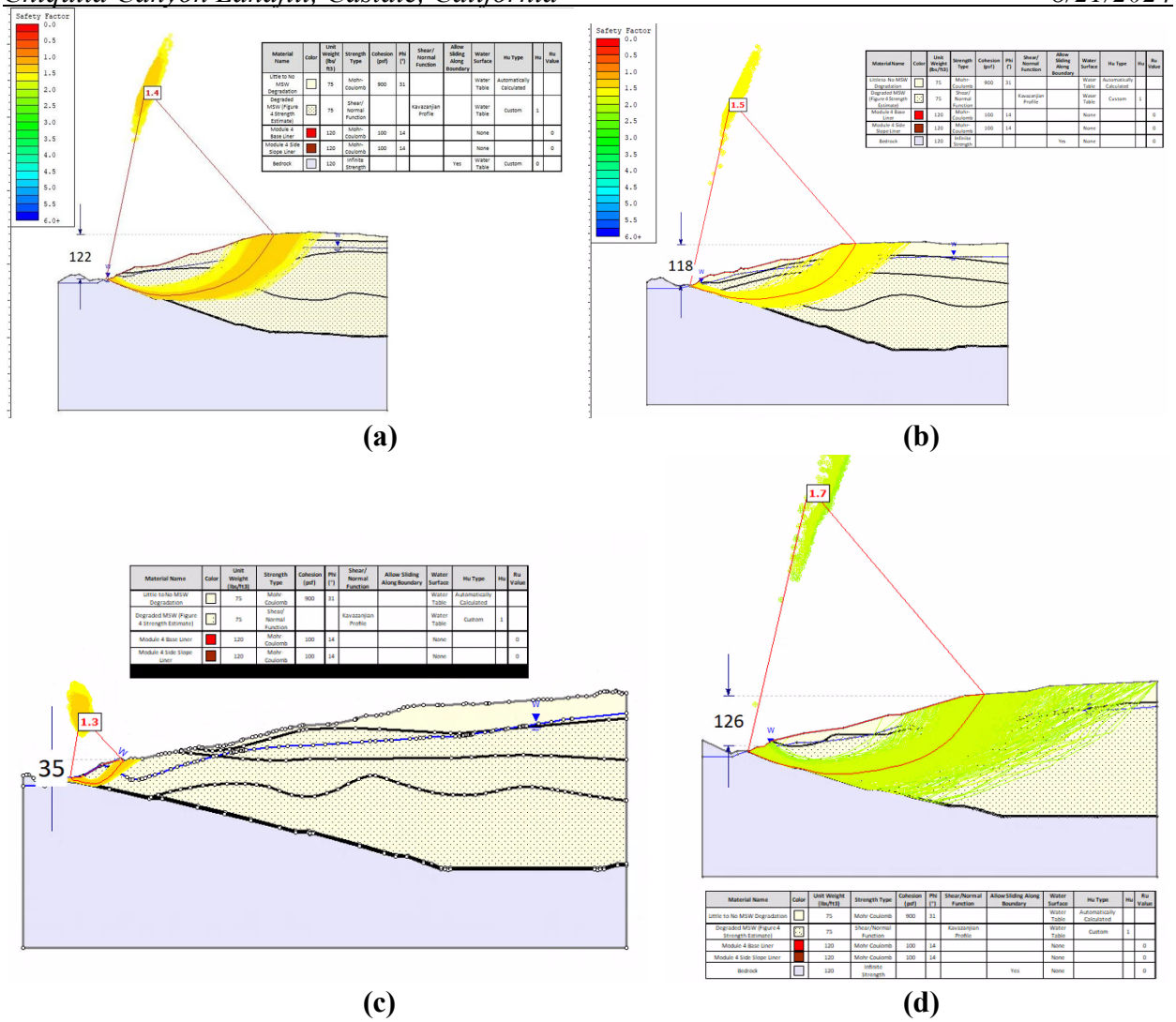


Figure 6. Values of static FoS and critical failure surfaces calculated using GLA input files for cross-sections: (a) WS-A, (b) WS-B, (c) WS-C, and (d) WS-D.

In addition, I used the slope stability input files provided by Richard A. Mitchell of GLA to conduct an inverse analysis of cross-sections WS-A and WS-B to determine the elevated pressure head that yields a static FoS of unity. These inverse analyses show only 12 ft of elevated liquid pressure is needed to reduce the static FoS for cross-sections WS-A and WS-B to unity, i.e., failure. The required or critical elevated liquid pressure is about 16 ft for cross-section WS-D. The critical failure surface for cross-section WS-C is a shallow surface near the toe of the slope (see) and thus is not impacted by elevated liquid pressures further upslope.

More importantly, if the waste and bottom liner system interface strengths are lowered as suggested above, the pressure head required to generate a FoS of unity will be less than 12 ft because these strengths are lower than the strengths used by GLA. Given field observations and the photograph in **Figure 5**, a pressure head of 12 ft could occur during the current SET Event.

Table 2 shows the static values of FoS are higher for the northern slope so a higher-pressure head is required than the western slope to generate a Fos of unity. Given the SET Event has moved towards the south, the northern slopes will probably remain stable.

TABLE 3. IMPACT OF ELEVATED LIQUID PRESSURES ON STATIC FOS

Cross-Section	Static FoS with 15 ft of Elevated Liquid Pressure
WS-A	0.9
WS-B	0.9
WS-C	1.2
WS-D	1.1

3.5 Findings and Recommendations

This section provides my review comments on the findings and recommendations presented by GLA in their May 2024 report titled: "West and North Slope Stability Analysis Update". My review comments on GLA's findings and recommendations are listed below:

1. GLA concludes the updated slope stability analyses show: "(i) the bulging movement that occurred on the western slope likely did not affect the liner system; and (ii) future sliding that could affect the liner is also unlikely under the conditions that were observed and the assumptions that were incorporated into the analyses."

   I disagree that the bulging movement along western slope did not affect the liner system as claimed by GLA. **Figure 7** is a photograph from Appendix F of the May 2024 GLA Slope Stability Report and it appears to show the geomembrane of the bottom liner system is torn (see red arrow). In addition, the blue arrow in **Figure 7** may also be indicating another tear in the geomembrane further south.



Figure 7. Photograph of exposed geomembrane during excavation of western slope toe (photo from Appendix F of May 2024 GLA Slope Stability Report).

I also disagree that "(ii) future sliding that could affect the liner is also unlikely under the conditions that were observed and the assumptions that were incorporated into the analyses." First, the critical failure surface in the following slope stability analyses in Appendix G of the GLA May 2024 report show the predicted critical failure surface will impact a portion of the bottom liner system:

1. NS-A (R1A).slmd
2. NS-B (R1A).slmd
3. NS-C (R1A).slmd
4. WS-B (R1A).slmd
5. WS-C (R1A).slmd
6. WS-D (R1A).slmd
7. WS-E (R1A).slmd

Second, only 12 ft of pressure head is needed to reduce the FoS to unity using GLA's elevated waste and geosynthetic interface strengths. If the waste and geosynthetic interface strengths recommended herein are used, the static FoS will decrease so a pressure head less than 12 ft will be need to reduce the FoS to unity. Therefore, I do not believe that future sliding could not affect the geomembrane in the bottom liner system.

2. I agree with GLA's conclusion that changing the leachate level can "significantly increase safety factors of the slope". This is true whether the leachate is lowered or raised. Given the presence of a SET Event, a rise in the leachate level is more likely due to the limited radius of influence of pumping in gas extraction wells. In addition, the decreased fluid level in gas wells CV-2352, CV-2351, and CV-2337 noted by GLA could be due to removal of condensate and/or perched leachate not overall lowering of the liquid/leachate level in the western slope.

3. I agree with GLA's conclusion that there are major uncertainties in their stability results due to: (1) charred waste strength and continuity, (2) elevated gas and liquid pressures, and (3) presence of perched leachate. To measure the liquid pressures, GLA should consider installing some Geokon high temperature piezometers that have a working range up to 480^0F as mentioned above. GLA can measure gas pressures at the gas wells using readily available equipment.

Summary and Recommendations

My main observation is there are significant uncertainties in the stability analyses presented in the May 2024 GLA Slope Stability Report. As a result, it may not be concluded the slopes are stable and will remain stable as the SET Event progresses.

Given the tension cracks that I observed during my site visit on May 23, 2024, the western slope was undergoing. This slope movement means the static factor of safety (FoS) of the slope is at or just above unity. In particular, Hussain and Stark (2011) show that slope movement and tension cracks start occurring in slopes when the FoS reduces to near 1.05. This information does not support the high values of static FoS reported by GLA in **Table 2** above. In particular, I think the static values of FoS for cross-sections WS-A, WS-B, WS-C, WS-D, and WS-E are less than 1.4, 1.5, 1.3, 1.7, and 1.8, respectively. Of course, the static FoS is changing as the SET Event moves south. GLA should focus on cross-sections south of the SET Event and establish the pre-SET Event FoS so when the SET Event arrives at that location, the decrease in FoS can be estimated based on observed slope movements. This will an provide insight to the mobilized waste strength and gas and liquid pressures present.

References

Hussain, M. and Stark, T.D. "Back-analysis of Preexisting Landslides". *Proc. of Specialty Conf. GEO-FRONTIERS 2011*, ASCE, Dallas, TX, March, 2011, pp. 3659-3668 at page 3660.

Huvaj, N. and Stark, T.D., (2008). "Back-Analysis of Landfill Slope Failures," *Proceedings of 6th International Conference on Case Histories in Geotechnical Engineering*, Arlington, VA, August 11-16, 2008, p. 276-286.

Jafari, N., Stark, T.D. and Merry, S.M., (2013). "10 July 2000 Payatas Landfill Slope Failure," *Intl. J. of Geoengineering Case Histories*, Intl. Soc. of Soil Mechanics and Geotechnical Engineering, Vol. 2(3), October, 2013, pp. 208-228; http://casehistories.geoengineer.org/volume/volume2/issue3/IJGCH_2_3_3.html, *doi: 10.4417/IJGCH-02-03-03*.

Jafari, N.H., Stark, T.D., and Thalhamer, T. (2017). "Progression of Elevated Temperatures in Municipal Solid Waste Landfills." *ASCE Journal of Geotechnical and Geoenvironmental Engineering*, 143(8), August, 2017, pp. 05017004-1 - 05017004-16, DOI: 10.1061/(ASCE)GT.1943-5606.0001683.

Lin, J., Stark, T.D., and Idries, A., (2024). "Extrapolating Residual GMX/GDC Interface Strength from Direct Shear Test Results," *Geosynthetics International Journal*, January, 2024, https://www.icevirtuallibrary.com/doi/abs/10.1680/jgein.23.00111.

Martin, J.W., Stark, T. D., Thalhamer, T., and Gerbasi, G.T. (2013). "Detection of Aluminum Waste Reactions and Associated Waste Fires," J. of Hazardous, Toxic, and Radioactive Waste, ASCE, July, 2013, 17(3), pp. 164-174.

Stark, T.D. and Poeppel, A.R. (1994). "Landfill Liner Interface Strengths from Torsional Ring Shear Tests," *Journal of Geotechnical Engineering*, ASCE, Vol. 120, No. 3, March, 1994, pp. 597-615.

Stark, T.D., Huvaj-Sarihan, N., and Li, G., (2009). "Shear Strength of Municipal Solid Waste for Stability Analyses," *Environmental Geology J.*, Springer Pub., http://dx.doi.org/10.1007/s00254-008-1480-0, 57(8), 2009, 1911-1923.

Stark, T.D., K. Akhtar, and Hussain, M., (2010). "Stability Analyses for Landfills Experiencing Elevated Temperatures," Proceedings of Specialty Conference GeoFlorida 2010: Advances in Analysis, Modeling and Design, ASCE, Orlando, FL, March 2010, 8 pp.